

Studies on the electronic structure of some cubic intermetallic compounds of dysprosium following the self-consistent augmented-plane-wave method

M. Belakhovsky

*Centre d'Etudes Nucléaires de Grenoble, B.P. 85, 38041 Grenoble Cedex, France
and Département de Recherche Fondamentale, Laboratoire de Chimie Physique Nucléaire, Grenoble, France*

D. K. Ray

*Laboratoire de Spectrométrie Physique, Université Scientifique et Médicale, B.P. 53, 38041 Grenoble Cedex, France
(Received 9 September 1974)*

The energy bands and the nature of the conduction electrons have been studied for two intermetallic compounds of dysprosium, i.e., DyZn and DyRh, following the self-consistent augmented-plane-wave (APW) method. The convergence of energy was found to be rapid for DyZn because the shell of $3d^{10}$ electrons for Zn lies below the conduction band. The Fermi energies (E_F) have been calculated to be 0.421 and 0.477 Ry for DyZn and DyRh, respectively. The densities and the numbers of conduction electrons inside and outside the APW spheres in each of these compounds are calculated, and it is shown that the character of conduction electrons inside the APW sphere of Dy is predominantly of d type. In order to see the accuracy of these results, self-consistent calculations were done for DyZn for different choices of the exchange potentials, and the calculated number of conduction electrons did not change significantly. The consequence of the predominance of d electrons in the conduction band on the various physical parameters is discussed.

I. INTRODUCTION

Much attention has been focused recently on the studies of intermetallic compounds of rare earths having CsCl structure.¹ The magnetic ordering has been found to change from antiferromagnetic to ferromagnetic as we go from compounds of rare earths with monovalent metals (Cu, Ag, Au) to divalent metals (Zr, Cd). Also, both DyZn and DyRh are ferromagnets, but their ordering temperatures are quite different, viz., 139 and 4.8 °K, respectively.^{2,3} DyZn has been found to have very large magnetic anisotropy,² and it undergoes cubic to tetragonal crystallographic transition at the ferromagnetic-ordering temperature.⁴ Moreover, the crystalline-electric-field parameters have been estimated for a number of rare-earth zinc and rhodium compounds by inelastic-neutron-scattering experiments.⁵ The free-electron model was found to be inadequate to explain the experimental results,⁶ and, consequently, the need to undertake calculations of the electronic structure of these compounds following a sophisticated method such as augmented plane wave (APW) has recently been pointed out.⁷ The results on energy bands on the structurally isomorphous compounds YZn and YCu have been reported earlier,⁷ but there are two principal uncertainties in these calculations. The choice of the initial configuration for Y was rather uncertain and the readjustment of charges between the two APW spheres was not taken into account. For removing these discrepancies it is necessary to do self-consistent APW calculations, the need for which has already been pointed out by Jan who found the band results to be not in good agreement

with the Fermi surface given by de Haas-van Alphen experiments.⁸ In this paper we report the results of our calculations on the two compounds of Dy, i.e., DyZn and DyRh, done following the self-consistent APW method.⁹⁻¹¹ A short account of this work has been published elsewhere.¹²

In order to explain the various physical observables in these compounds, the calculations of energy bands alone are not sufficient, and it is necessary to evaluate the electronic functions in the metallic state. These functions can then be used to estimate the contributions of the conduction electrons—direct and indirect—to all physical parameters. Similar calculations have recently been done by Das and Ray¹³ who estimated the direct contribution of the conduction electrons to the crystalline-electric-field (CEF) parameters and the charge density at the nucleus for dysprosium metal.¹⁴ But the accuracy of these results is rather uncertain since no test was made to see the convergence of the electronic densities with various cycles of iteration and also for various choices of the exchange potential. So we have followed here the self-consistent APW method to calculate the energy bands and the wave functions of the conduction electrons for DyZn and DyRh and have tested the accuracy of our results from the convergence of the results for different choices of the parameter α in the Slater exchange potential.¹⁵ The convergence has been found to be fairly rapid for DyZn. Only five iterations were found to be sufficient, whereas for DyRh we had to go to nine cycles. The numbers of each type of conduction electrons s , p , d , f , etc., inside the APW spheres have been calculated, and these numbers do not depend sensitively on the choice of

α . The most significant result of these calculations is the predominance of d electrons inside the APW sphere of Dy, which must be related to the failure of the simple Ruderman-Kittel-Kasuya-Yosida (RKKY) model¹⁶ and the large observed magnetic anisotropy in DyZn.²

II. CALCULATIONS OF ENERGY BANDS AND CHARACTERS OF CONDUCTION ELECTRONS

The central problem in any APW band calculation is the construction of the muffin-tin potential. The initial muffin-tin potential for our problem here has been constructed from the atomic wave function of Dy, Zn, and Rh as obtained from the Hartree-Fock-Slater (HFS) solution. The choice of initial atomic configuration for Dy is important. The ground atomic configuration for Dy is $(4f)^{10}(6s)^2$, but in all compounds of Dy—whether metal or insulator—there are nine electrons in the $4f$ shell.^{17,18} So we have done our calculations with the $(4f)^9(6s)^2(5d)^1$ configuration. Since the $4f$ electrons were found to lie entirely within the APW sphere of Dy we treated these as core electrons. But instead of treating the core electrons as frozen we solved the Schrödinger equations corresponding to these electrons in the presence of the spherically symmetric part of the muffin-tin potential by the HFS method. In this way we introduce to some extent the effect of the crystal potential on the core electrons. As has been discussed by Freeman,¹⁷ considerable error might be introduced if one tries to do band calculations for the $4f$ electrons because of the large intra-atomic Coulomb and exchange potential for $4f$ electrons arising from their localized character. Also, the radial functions for $4f$ electrons are practically zero near the APW sphere, and consequently the condition of matching of wave functions on the APW sphere involved in the APW method would lead to numerical inaccuracies in the band calculations for $4f$ electrons. The outer atomic configurations used for Zn and Rh were $(4s)^2$ and $(4d)^8(5s)^1$, respectively. The exchange potential was taken in the localized form of Slater, i. e., $V_{ex} = -3\alpha[(3/\pi)\rho(r)]^{1/3}$ with different choices of α . As has been discussed by Slater,¹⁵ the value of α in the case of solids should be in between 1 and $\frac{2}{3}$. Therefore we have done our calculations for $\alpha=1$, 0.92, 0.83, and 0.75 for the case of DyZn and $\alpha=1$ for DyRh. The initial muffin-tin potential and the density $\rho(r)$ were constructed following the method discussed in detail by Loucks.¹⁹ The APW function at any point \vec{k} inside the reduced Brillouin zone and corresponding to an energy E is given by

$$\begin{aligned} \Phi_{\vec{k}}(E, \vec{r}) &= \frac{1}{F_{\vec{k}}(E)} \sum_{\vec{k}_n} C_{\vec{k}}(\vec{k}_n, E) \Psi(\vec{k}_n, E, \vec{r}) \\ &= \sum_{\vec{k}_n} D_{\vec{k}}(\vec{k}_n, E) \Psi(\vec{k}_n, E, \vec{r}), \end{aligned} \quad (1)$$

where $\vec{k}_n = \vec{k} + \vec{K}_n$, \vec{K}_n being any reciprocal-lattice vector; $C_{\vec{k}}(\vec{k}_n, E)$ is the coefficient of mixing of the n th APW function Ψ in the total APW function Φ ; and $F_{\vec{k}}(E)$ is the appropriate normalization vector. The $D_{\vec{k}}(\vec{k}_n, E)$'s are the normalized mixing coefficients. The individual APW function $\Psi(\vec{k}_n, E, \vec{r})$ is given by

$$\begin{aligned} \Psi|\vec{k}_n, E, \vec{r}| &= \delta_1 e^{i\vec{k}_n \cdot \vec{r}} + \delta_2 \sum_s e^{i\vec{k}_n \cdot \vec{r}_s} \\ &\times 4\pi \sum_{l,m} i^l \frac{J_l(l|\vec{k}_n|\sigma_s)}{R_l(E, \sigma_s)} Y_l^{m*}(\vec{k}_n) Y_l^m(\vec{\rho}) R_{sl}(E, \rho), \end{aligned} \quad (2)$$

where E denotes the energy eigenvalue, \vec{r} is the coordinate with respect to the center of the coordinate system, \vec{r}_s is that of the s th atom with respect to the same center, and $\vec{\rho} = \vec{r} - \vec{r}_s$. The radius of the s th APW sphere is given by σ_s . The δ_1 part exists only outside the APW spheres, whereas the δ_2 part is nonvanishing inside the APW spheres. $R_{sl}(E, \rho)$ is the radial function which is given by the solution of the Schrödinger equation for the s th atom, i. e.,

$$\left[-\frac{1}{\rho^2} \frac{d}{d\rho} \left(\rho^2 \frac{d}{d\rho} \right) + \frac{l(l+1)}{\rho^2} + V_s(\rho) \right] R_{sl}(E, \rho) = ER_{sl}(E, \rho), \quad (3)$$

where $V_s(\rho)$ is the spherically symmetric part of the muffin-tin potential inside the s th APW sphere. The radii of the APW spheres were so adjusted until one gets the largest amount of electrons inside the spheres. Values of these radii and other structural parameters are given in Table I. The potential (Coulomb plus exchange) did not vary significantly outside the APW spheres, indicating that the non-muffin-tin part of the potential is not important in the present calculations. The origin of the energy bands was taken with respect to the average potential outside the APW spheres.

Using values of 1 up to 10, the energy eigenvalues and the corresponding coefficients $C_{\vec{k}}(\vec{k}_n, E)$ were determined by solving the determinant of the total Hamiltonian between the APW functions $\Psi(\vec{k}_n, E, \vec{r})$. A basis set of 33 reciprocal-lattice vectors or more, depending on the \vec{k} point in the reduced Brillouin zone, was used in order to insure a convergence in eigenvalues of about 0.002 Ry. Owing to the high symmetry O_h^1 , no general point was included, and it was on the other hand necessary to use a symmetrized version of the APW formalism, as developed by F. Perrot. The convergence in the self-consistent procedure has been tested through the variation in orbital d -character density of the conduction band in the final iteration, which is 0.003 a. u.⁻³. The normalization factors $F_{\vec{k}}(E)$ were then determined from the relation

$$F_{\vec{k}}(E)^2 = \sum_{n,m} C_{\vec{k}}(\vec{k}_n, E) C_{\vec{k}}(\vec{k}_m, E) \Delta_{nm}(\vec{k}, E), \quad (4)$$

where the overlap factor $\Delta_{mn}(\vec{k}, E)$ is given by

$$\begin{aligned} \Delta_{mn}(E) &= \langle \Psi(\vec{k}_m, E, \vec{r}) | \Psi(\vec{k}_n, E, \vec{r}) \rangle \\ &= \Omega_0 \left[\delta(\vec{k}_m, \vec{k}_n) - \frac{1}{\Omega_0} 4\pi \sum_s \sigma_s^2 e^{i(\vec{k}_m - \vec{k}_n) \cdot \vec{r}_s} \frac{J_1(|\vec{k}_m - \vec{k}_n| \sigma_s)}{|\vec{k}_m - \vec{k}_n|} \right. \\ &\quad \left. + \sum_{l=0}^{\infty} (2l+1) J_l(|\vec{k}_m| \sigma_s) J_l(|\vec{k}_n| \sigma_s) P_l(\hat{k}_m \cdot \hat{k}_n) \frac{\delta}{\delta E} \left(\frac{R'_{sl}(E, \sigma_s)}{R_{sl}(E, \sigma_s)} \right) \right], \end{aligned} \quad (5)$$

where Ω_0 is the volume of the unit cell; R'_{sl} is the derivative of the radial function R_{sl} . At first we used 56 nonequivalent \vec{k} points in the reduced zone, which correspond to 1000 points in the full Brillouin zone. Subsequently for carrying out self-consistent calculations we changed this number to 64 points. From the values of $C_{\vec{k}}(\vec{k}_n, E)$ and $F_{\vec{k}}(E)$ the normalized mixing coefficients $D_{\vec{k}}(\vec{k}_n, E)$ were determined. These coefficients were then used to get the spherically symmetric part of the electronic densities inside and outside the APW spheres, expressions for which are given by

$$\begin{aligned} \rho_s^{\text{in}}(r) &= 2 \left(\sum_{\vec{k}, E} \sum_{m, n} e^{i(\vec{k}_m - \vec{k}_n) \cdot \vec{r}_s} D_{\vec{k}}(\vec{k}_m, E) D_{\vec{k}}(\vec{k}_n, E) \right. \\ &\quad \left. \times \sum_{l=0}^{\infty} (2l+1) J_l(|k_n| \sigma_s) J_l(|k_m| \sigma_s) P_l(\hat{k}_m \cdot \hat{k}_n) \frac{R_{sl}^2(E, r)}{R_{sl}^2(E, \sigma_s)} \right), \end{aligned} \quad (6)$$

$$\rho^{\text{out}}(r) = 2 \sum_{\vec{k}, E} \sum_{m, n} D_{\vec{k}}(\vec{k}_n, E) D_{\vec{k}}(\vec{k}_m, E) J_0(|\vec{K}_m - \vec{K}_n| r), \quad (7)$$

where the summation over \vec{k} and E include all occupied states. From Eq. (7), the charge density outside the spheres is not constant but varies with distance r when more than one reciprocal vector \vec{k}_n is used. The number of conduction electrons inside and outside the APW spheres is obtained by integrating the respective densities, and these are given by

$$\begin{aligned} N_s(\text{inside APW sphere}) &= -8\pi \sigma_s^2 \sum_{\vec{k}, E} \sum_l (2l+1) \sum_{n, m} e^{i(\vec{k}_m - \vec{k}_n) \cdot \vec{r}_s} D_{\vec{k}}(\vec{k}_n, E) \\ &\quad \times D_{\vec{k}}(\vec{k}_m, E) J_l(|\vec{k}_n| \sigma_s) J_l(|\vec{k}_m| \sigma_s) P_l(\hat{k}_m \cdot \hat{k}_n) \frac{\delta}{\delta E} \left(\frac{R'_{sl}(E, \sigma_s)}{R_{sl}(E, \sigma_s)} \right), \end{aligned} \quad (8)$$

$$N(\text{outside}) = 2\Omega_0 \sum_{\vec{k}, E} \sum_{m, n} D_{\vec{k}}(\vec{k}_m, E) D_{\vec{k}}(\vec{k}_n, E) \left(\delta(\vec{k}_m, \vec{k}_n) - \sum_s \frac{4\pi \sigma_s^2}{\Omega_0} e^{i(\vec{k}_m - \vec{k}_n) \cdot \vec{r}_s} \frac{J_1(|\vec{k}_m - \vec{k}_n| \sigma_s)}{|\vec{k}_m - \vec{k}_n|} \right). \quad (9)$$

The self-consistent APW calculations were then carried out following the procedure given by Mattheiss *et al.*⁹ Using the core functions and the electronic density calculated by the APW method, the new charge density inside and outside the APW spheres were calculated. These new charge densities were then used to evaluate the new muffin-tin potential. The exchange part of the potential is directly given from the expression for the Slater potential constructed from the new charge density. The Coulomb potential inside the APW spheres was obtained in the usual way by integrating Poisson's equation. The total charge in the crystal can now be conceived to be consisting of effective charges Q_{eff} located at the various atomic sites and a uniform background of negative charge density extending throughout the crystal. For calculating the constant part of the Coulomb potential due to these effective charges inside the APW spheres and also the average potential outside the APW spheres we have solved the Madelung problem following the procedure given by Slater and De Cicco for the fcc

lattice.²⁰ In this way the new muffin-tin potential $V^{\text{new}}(r)$ is constructed.

For doing the successive iteration procedure we

TABLE I. Values of different parameters involved in the APW calculations for DyZn and DyRh.

	Compound	
	DyZn	DyRh
Structure-type	CsCl(B_2)	CsCl(B_2)
space group	O_h^1	O_h^1
Lattice parameter (a)	6.736 a. u.	6.438 a. u.
Dysprosium APW sphere radius	3.151 a. u.	3.1035 a. u.
Zinc and rhodium APW sphere radius	2.6825 a. u.	2.73 a. u.
Average potential outside APW spheres	-0.140 Ry	-0.119 Ry

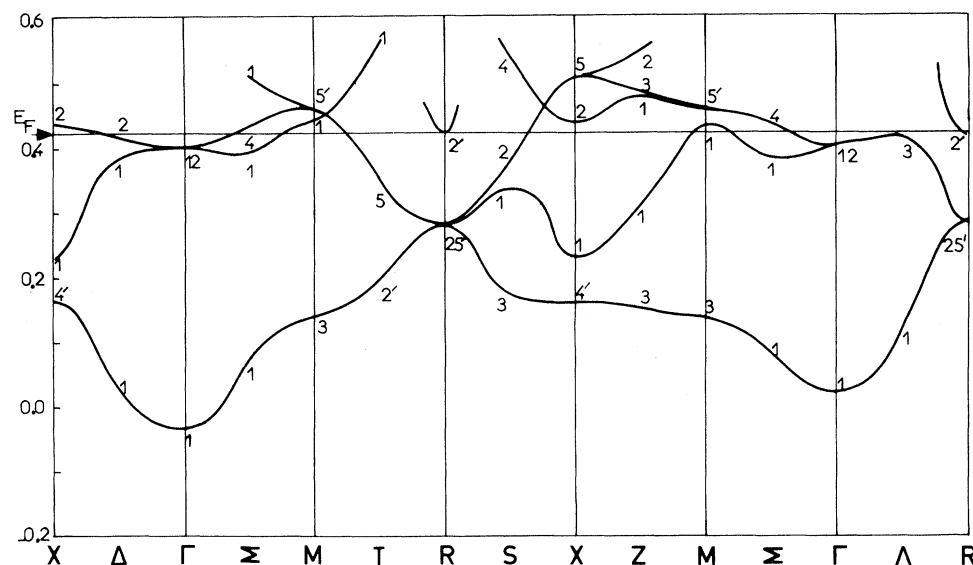


FIG. 1. Self-consistent bands for DyZn after fifth iteration with $\alpha = 1$.

took the muffin-tin potential using the following prescription:

$$V(r) = \beta V^{\text{old}}(r) + (1 - \beta) V^{\text{new}}(r). \quad (10)$$

The convergence of energy with successive iterations depends on the value of β used. For DyZn we found that $\beta = 0.70$ for all successive iterations gave quick convergence of energy. But for DyRh we had to use different values of β in different iterations to get reasonable convergence of energy.

A. Results for DyZn

The results of energy bands for DyZn obtained after the fifth iteration using $\alpha = 1$ are given in Fig.

1. The convergence of energy for successive iterations is given in Table II for some k values and representations. It is evident from these results that after second iteration (i. e., after band functions are used to generate the potential) the energy does not vary significantly. Also, it is to be noted that the d bands of Zn lie below the conduction bands and consequently are not shown in the Fig. 1. Using Eqs. (8) and (9) we have estimated the number of each type of conduction electrons inside the two APW spheres for each iteration, and these are given in Table III. The actual and effective charges inside the APW spheres as well as the Fermi energy E_F are indicated in the same table. The con-

TABLE II. Values of energies in Ry corresponding to some k points and representations for successive iterations in DyZn.

k values in $2\pi/a$ units	Representations	Energies in Ry for successive iterations				
		1	2	3	4	5
(0, 0, 0)	Γ_1	-0.026	-0.031	-0.033	-0.034	-0.035
	Γ_{12}	0.384	0.394	0.397	0.398	0.398
(0, 25, 0, 0)	Δ_1	0.036	0.031	0.029	0.028	0.027
	Δ_1	0.375	0.379	0.380	0.380	0.380
	Δ_2	0.401	0.413	0.415	0.416	0.417
(0.5, 0, 0)	X_1	0.228	0.230	0.230	0.230	0.230
	X_1'	0.175	0.167	0.163	0.162	0.161
	X_2	0.419	0.432	0.435	0.436	0.436
	X_5	0.500	0.510	0.511	0.512	0.512
(0.5, 0.5, 0)	M_1	0.428	0.438	0.440	0.441	0.442
	M_3	0.147	0.143	0.141	0.140	0.139
	M_5'	0.467	0.464	0.463	0.462	0.462
(0.5, 0.5, 0.5)	R_{25}'	0.281	0.285	0.285	0.285	0.285
	R_2'	0.445	0.430	0.425	0.422	0.421

TABLE III. Results showing the characters of electrons inside the APW spheres of DyZn for successive iterations. The values of real charge, effective charge, and Fermi energy are also given. All the results are for $\alpha = 1$.

Results on	First iteration		Second iteration		Third iteration		Fourth iteration		Fifth iteration		
	Dy	Zn	Dy	Zn	Dy	Zn	Dy	Zn	Dy	Zn	
Number of electrons of type	<i>s</i>	0.282	0.870	0.280	0.922	0.279	0.930	0.279	0.934	0.278	0.936
	<i>p</i>	0.226	0.570	0.227	0.596	0.226	0.604	0.226	0.608	0.226	0.609
	<i>d</i>	1.575	0.063	1.488	0.060	1.472	0.059	1.465	0.059	1.462	0.059
	<i>f</i>	0.022	0.005	0.025	0.004	0.025	0.004	0.026	0.004	0.026	0.004
Real charge		0.890 <i>e</i>	0.487 <i>e</i>	0.974 <i>e</i>	0.413 <i>e</i>	0.991 <i>e</i>	0.398 <i>e</i>	0.999 <i>e</i>	0.391 <i>e</i>	1.00 <i>e</i>	0.387 <i>e</i>
Effective charge		2.816 <i>e</i>	1.675 <i>e</i>	2.915 <i>e</i>	1.610 <i>e</i>	2.934 <i>e</i>	1.597 <i>e</i>	2.943 <i>e</i>	1.590 <i>e</i>	2.947 <i>e</i>	1.587 <i>e</i>
Average potential outside APW spheres		-0.143 Ry		-0.141 Ry		-0.140 Ry		-0.140 Ry		-0.140 Ry	
E_F		0.419 Ry		0.430 Ry		0.425 Ry		0.422 Ry		0.421 Ry	

vergence of the number of electrons inside the APW spheres is evidently very good. The most important point to be noted out of these results is that *d* electrons constitute about 72% of the electrons inside the Dy APW spheres. Also, the electrons are fairly well localized inside the APW spheres, only 28% lying outside.

We next studied how these results depend on the choice of the parameter α in the exchange potential. Since the Slater exchange potential incorporates the exchange and to some extent the correlation interaction as well, the value of α in the case of solids is not definite but it should lie between 1 and $\frac{2}{3}$ (the

Kohn-Sham value).¹⁵ We have, therefore, done calculations for $\alpha = 1.0, 0.92, 0.83,$ and 0.75 . Below the value of 0.75 for α , the *d* band of zinc appears inside the conduction band, and there is no experimental evidence for this in the case of DyZn. We have studied the energy bands and the numbers of electrons inside the APW spheres for different values of α . The converged energy values at some points in the reduced zone and for some values of α are given in Table IV. The results indicate that except for Γ_1 (for which the energy decreases) there is a small increase in energy with decrease in the value of α . The numbers of electrons inside

TABLE IV. Values of energies corresponding to some *k* points and representations for three values of α in DyZn.

<i>k</i> -values in units of $2\pi/a$	Representations	Energies in Ry for α		
		1.0	0.92	0.75
(0, 0, 0)	Γ_1	-0.035	-0.026	-0.002
	Γ_{12}	0.398	0.416	0.458
(0.25, 0, 0)	Δ_1	0.027	0.037	0.064
	Δ_1	0.380	0.394	0.430
(0.5, 0, 0)	X_4'	0.161	0.174	0.212
	X_1	0.230	0.239	0.260
	X_2	0.436	0.453	0.491
(0.5, 0.5, 0)	M_3	0.140	0.153	0.191
	M_3'	0.462	0.472	0.497
(0.5, 0.5, 0.5)	R_{25}'	0.286	0.297	0.322
	R_2'	0.421	0.435	0.476
(0.25, 0.25, 0.25)	Λ_1	0.115	0.126	0.154
	Λ_3	0.415	0.429	0.463

TABLE V. Characters of electrons inside the APW spheres for different choices of α .

Number of electrons of type	$\alpha=1$		$\alpha=0.92$		$\alpha=0.75$	
	Dy	Zn	Dy	Zn	Dy	Zn
<i>s</i>	0.279	0.936	0.279	0.931	0.278	0.899
<i>p</i>	0.227	0.610	0.231	0.620	0.240	0.634
<i>d</i>	1.462	0.059	1.425	0.069	1.343	0.136
<i>f</i>	0.025	0.0048	0.027	0.0050	0.031	0.005

the APW spheres do not sensitively depend on α , as will be evident from Table V.

B. Results for DyRh

Since the shell $(4d)^8$ of Rh is incomplete and since the atomic $4d$ function extends beyond the radius of the APW sphere of Rh, it is necessary to consider the $4d$ electrons of Rh within the band calculations. This introduces relatively more uncertainty in the calculated results because of the large intra-atomic correlation for the $4d$ electrons. Also, since the $4d$ shell is incomplete there is considerable mixing of these electrons with other electrons, and consequently the dispersion for these bands is large and the convergence of energy is slow. In order to achieve quicker convergence we varied the value of β in successive iterations. We had to go to ninth iteration to get fairly good convergence of energy. The energy bands after the ninth iteration are given in Fig. 2.

In Table VI the convergence of energy is given for the last four iterations at some points in the reduced zone. The number of electrons of each character inside the APW spheres is presented in Table VII for the last three iterations. The values of the effective charges Q_{eff} and the Fermi energy E_F are also indicated in this table. The number of d electrons inside the Dy APW sphere is 65% of the total

TABLE VI. Values of energies in Ry in DyRh for some representations corresponding to the last four iterations (sixth-ninth).

Representations	6	7	8	9
Γ_1	0.143	0.148	0.147	0.147
Γ_{12}	0.148	0.187	0.180	0.183
M_1	0.166	0.209	0.201	0.205
M_3	0.154	0.185	0.179	0.182
M_4	0.318	0.389	0.375	0.382
M_5	0.217	0.267	0.257	0.262
X_1	0.359	0.356	0.356	0.355
X_2	0.485	0.468	0.471	0.468

number of electrons inside, which is a little less than in the case of DyZn. This is presumably owing to the fact that the d bands below the Fermi energy are principally due to the electrons of Rh. There is, on the other hand, much more localization of electrons inside the APW spheres in this case, only about 9% lying outside the APW spheres compared with the value of 28% for the case of DyZn.

III. DISCUSSION

In the band results presented in the Sec. II no account has been taken of the spin-dependent exchange,^{21,22} which one should consider in the magnetically ordered phase. So our band results are in principle valid for the high-temperature paramagnetic phases of these compounds. For a better description of the higher bands in the ferromagnetic phase it will be worthwhile to consider the exchange to be spin dependent. Also, it will be interesting to include the effect of the spin-orbit interaction on the bands near the Fermi surface, since the relativistic effects are important for the rare earths.¹⁷

The most important result that one obtained from

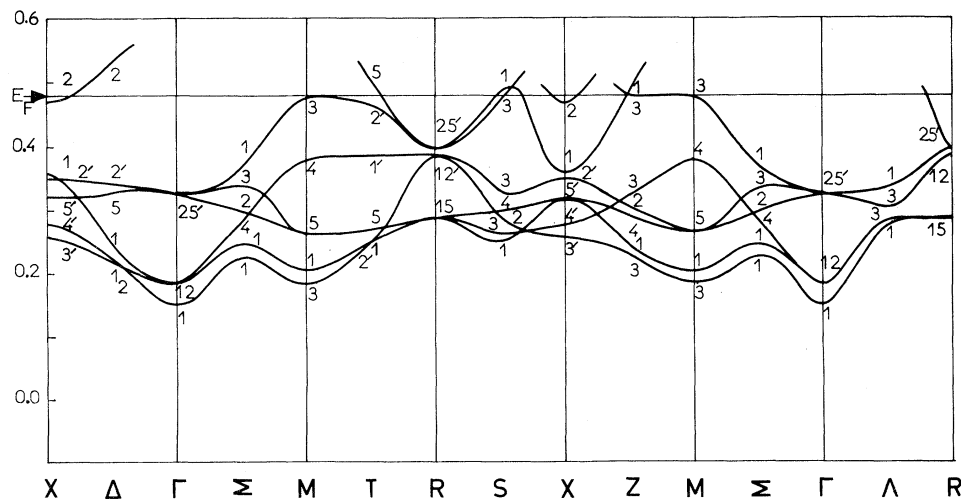


FIG. 2. Self-consistent bands for DyRh after ninth iteration with $\alpha=1$.

TABLE VII. Results showing the characters of electrons, the effective charges, and Fermi energy for the last three iterations in DyRh.

Results on		Seventh iteration		Eighth iteration		Ninth iteration	
		Dy	Rh	Dy	Rh	Dy	Rh
Number of electrons of type	s	0,313	0,517	0,308	0,515	0,311	0,513
	p	0,284	0,166	0,275	0,162	0,278	0,164
	d	1,38	8,07	1,32	8,17	1,35	8,12
	f	0,088	0,95	0,085	0,014	0,086	0,015
	Q_{eff}	3,36	1,90	3,38	1,77	3,36	1,84
	E_f	0,480		0,474		0,477	

the values presented in Sec. II is the structure of the d band and the predominance of the d electrons inside the rare-earth APW sphere. First, there is a fairly large splitting of the d band, which is evident from the fact that only Γ_{12} lies below the Fermi energy for DyZn, Γ'_{25} lying about 0.3 Ry above it. There will then be fairly a large contribution to the CEF parameters from the aspherical d electrons lying inside the Dy APW sphere. In the case of DyRh, on the other hand, the d bands are primarily from d electrons lying inside the Rh APW sphere and consequently the d -electronic contribution from the Dy APW sphere is expected to be less than in the case of DyZn.

The presence of a large amount of d electrons in the rare-earth APW sphere would modify considerably the applicability of the usual model developed on the basis of plane waves for conduction electrons to describe the exchange interaction in the rare earths. The predominance of the d electrons particularly near the Fermi surface would cause the following effects:

(i) Both the isotropic and the anisotropic parts of the exchange would be mainly determined by the d electrons. The experimental values of exchange parameters for DyZn and DyRh are not yet available. Ray²³ has recently calculated the exchange integrals between the $4f$ and conduction electrons using APW functions and obtained value of the isotropic part of the exchange fairly close to that given by Buschow *et al.*²⁴ for GdZn. The negative contribution from the conduction electrons to the quadrupole coupling as obtained by Belakhovsky and Pierre²⁵ from Mössbauer experiments on DyZn also indicate the predominance of d electrons in the conduction band.

(ii) The hyperfine fields on the rare-earth and

non-rare-earth sites in GdZn have been measured by Oppelt *et al.*²⁶ Subtracting the core polarization terms from the experimental values of the hyperfine fields, one gets²⁷ the ratio of the hyperfine fields at Gd and Zn sites to 1:2. Sakurai²⁷ has recently calculated these fields on the basis of the usual RKKY model, which uses plane waves for the conduction electrons, and obtained a ratio of 30:1 at the two sites, thus indicating that the nature of conduction electrons is very different from the plane waves near the nuclear sites. It should be noted in this connection that the spin polarization of the conduction electrons has recently been measured by neutron experiments for Gd metal,²⁸ and these results are quite different from what one expects from the simple RKKY model.²⁹

(iii) The anisotropic part of the exchange is expected to be large if the d electrons predominate as is evident from the calculations of Ray.²³ For DyZn the magnetic anisotropy has already been found to be large² indicating the importance of anisotropic exchange. In fact, the general problem of the anisotropy of exchange in rare-earth metals and intermetallic compounds is now of great interest.³⁰ The spin-wave spectra of Dy metal have indicated the importance of the anisotropic exchange in removing degeneracies.³¹ Lindgard *et al.*³² have studied earlier the effect of the anisotropic exchange on the magnon dispersion for terbium. But these results and conclusions can only be meaningful if one takes into account the realistic conduction electronic functions and nonspherical Fermi surface.

(iv) In addition to the linear exchange, the d electrons in the conduction band would cause an appreciable biquadratic exchange as well.²³ Such biquadratic exchange might be responsible for the observed crystallographic transition from cubic to tetragonal structures for DyZn. Similar structural transition has been observed earlier on the intermetallic compound DySb,^{33,34} and Levy³⁴ proposed that biquadratic exchange which is responsible for the phase transition might be partly due to the conduction electrons.

ACKNOWLEDGMENTS

The authors are grateful to Dr. F. Perrot of CEA LIMEIL for making the self-consistent APW program available to them. It is a pleasure to thank Dr. J. Pierre for discussions and his interest in the work.

¹J. Pierre and R. Pauthenet, C. R. Acad. Sci. (Paris) **260**, 2739 (1965); R. E. Walline and W. E. Wallace, J. Chem. Phys. **41**, 3285 (1964); **42**, 604 (1965); G. T. Alfieri, E. Banks, K. Kanematsu, and T. Ohoyanna, J. Phys. Soc. Jpn. **23**, 507 (1967); K. Kanematsu, G. T. Alfieri, and E. Banks, *ibid.* **26**, 244 (1969); J. W.

Cable, W. C. Koehler, and E. O. Wollan, Phys. Rev. **136**, A240 (1964); for other references see Ref. 3.

²P. Morin and J. Pierre, Phys. Status Solidi A **17**, 479 (1973).

³R. Chamard-Bois, Nguyen van Nhung, J. Hakinthos, and M. Wintenberger, Solid State Commun. **10**, 685 (1972).

- ⁴J. Pierre (private communication).
- ⁵R. Chamard-Bois, J. Rossat-Mignod, K. Knorr, and W. Drexel, *Solid State Commun.* **13**, 1549 (1973); P. Morin, J. Pierre, J. Rossat-Mignod, K. Knorr, and W. Drexel, *Phys. Rev. B* **9**, 4932 (1974); K. Knorr, W. Drexel, R. Chamard-Bois, J. Rossat-Mignod, P. Morin, and J. Pierre, in *Proceedings of the Conference on Crystalline Electric Field Effects in Metals and Alloys*, Montreal, Canada, 1974 (unpublished).
- ⁶J. Pierre, *Solid State Commun.* **7**, 165 (1969).
- ⁷M. Belakhovsky, J. Pierre, and D. K. Ray, *Phys. Rev. B* **6**, 939 (1972).
- ⁸J. P. Jan, *Phys. Rev. B* **8**, 3590 (1973).
- ⁹L. F. Mattheiss, J. H. Wood, and A. C. Switendick, in *Metals in Computational Physics*, edited by B. Alder, S. Fernbach, and M. Rotenberg (Academic, New York, 1968), Vol. 8, p. 63.
- ¹⁰E. C. Snow and J. T. Waber, *Phys. Rev.* **157**, 570 (1967).
- ¹¹D. A. Papaconstantopoulos, J. R. Anderson, and J. W. McCaffrey, *Phys. Rev. B* **5**, 1214 (1972), and the references therein.
- ¹²D. K. Ray and M. Belakhovsky, *Phys. Rev. Lett.* (to be published).
- ¹³K. C. Das and D. K. Ray, *Solid State Commun.* **8**, 2025 (1970).
- ¹⁴K. C. Das and D. K. Ray, *Solid State Commun.* **9**, 1061 (1971).
- ¹⁵J. C. Slater and K. H. Johnson, *Phys. Rev. B* **5**, 844 (1972), and the references therein.
- ¹⁶M. A. Rudermann and C. Kittel, *Phys. Rev.* **96**, 99 (1954); T. Kasuya, *Prog. Theor. Phys.* **16**, 45 (1956); K. Yoshida, *Phys. Rev.* **106**, 893 (1957).
- ¹⁷A. J. Freeman, in *Magnetic Properties of Rare Earth Metals*, edited by R. J. Elliott (Plenum, London, 1972), p. 245.
- ¹⁸K. N. R. Taylor and M. I. Darby, *Physics of Rare Earth Solids* (Chapman and Hall, London, 1972), p. 1.
- ¹⁹T. L. Loucks, *Augmented Plane Wave Method* (Benjamin, Amsterdam, 1967).
- ²⁰J. C. Slater and P. Decicco, MIT Solid State and Molecular Theory Group, *Quart. Progr. Rept. No. 50*, 1963 (unpublished).
- ²¹A. J. Freeman and R. E. Watson, *Phys. Rev.* **127**, 2058 (1962).
- ²²J. O. Dimmock, *Solid State Phys.* **26**, 103 (1971).
- ²³D. K. Ray, *Solid State Commun.* (to be published).
- ²⁴K. H. J. Buschow, A. Oppelt, and E. Dormann, *Phys. Status Solidi B* **50**, 647 (1972).
- ²⁵M. Belakhovsky and J. Pierre, *Solid State Commun.* **9**, 1409 (1971).
- ²⁶A. Oppelt, E. Dormann, and K. H. J. Buschow, *Phys. Status Solidi B* **51**, 275 (1972).
- ²⁷J. Sakurai (private communication).
- ²⁸R. M. Moon, V. C. Koehler, J. W. Cable, and H. R. Child, *Phys. Rev. B* **5**, 997 (1972).
- ²⁹B. Harmon and A. J. Freeman, *Phys. Rev. B* **10**, 1979 (1974); **10**, 4849 (1974).
- ³⁰R. J. Elliott, in *Ref. 17*, p. 1, and the references therein.
- ³¹R. M. Nicklow and W. Wakabayashi, in *Proceedings of Fifth IAEA Symposium on Neutron Inelastic Scattering*, Grenoble, 1972 (unpublished).
- ³²P. A. Lindgard, A. Kowalska, and P. Laut, *J. Phys. Chem. Solids* **28**, 1357 (1967).
- ³³F. Levy, *Phys. Kondens. Mater.* **10**, 86 (1969).
- ³⁴P. M. Levy, *Phys. Rev. Lett.* **27**, 1385 (1971); *AIP Conf. Proc.* **5**, 373 (1972).